Submitted to The Astrophysical Journal (April 2, 2004)
Preprint typeset using LaTeX style emulateapj v. 5/14/03

A COMPREHENSIVE STUDY OF YOUNG BLACK HOLE POPULATIONS

Krzysztof Belczynski[1,2], Aleksander Sadowski[3], Frederic A. Rasio[1]
[1] Northwestern University, Dept of Physics and Astronomy, 2145 Sheridan Rd, Evanston, IL 60208
[2] Lindheimer Postdoctoral Fellow
[3] Warsaw University, Dept. of Physics, Hoza 69, 00-681, Warsaw, Poland
belczynski, rasio@northwestern.edu; oleks@camk.edu.pl
Submitted to The Astrophysical Journal (April 2, 2004)

ABSTRACT

We present theoretical models of black hole (BH) populations in young stellar environments, such as starbursts and young star clusters. Using a population synthesis approach we compute the formation rates and characteristic properties of single and binary BHs for various representative ages and choices of parameters. We find that most of the BHs (typically 80% for an initial 50% binary fraction) are single, but with many originating from primordial binaries (which either merged into a single massive star or were disrupted following a supernova explosion). A smaller but significant fraction (typically 20%) of the BHs remain in binary systems. Main-sequence stars are the most frequent BH companions, but massive BH–BH binaries are the next most numerous group. The most massive BHs found in our simulations reach $\sim 80\,M_\odot$, and are formed through mergers of massive binary components. If formed in a dense star cluster such a massive stellar BH may become the seed for growth to a more massive ("intermediate-mass") BH. Although we do not include dynamical interactions, our results provide realistic initial conditions for N-body simulations of dense star clusters (e.g., globular clusters) including primordial BHs.

Subject headings: binaries: close — black hole physics — gravitational waves — stars: evolution

1. INTRODUCTION

Until recently it was believed that BHs existed in two separate mass ranges: stellar-mass BHs, with masses $\sim 10\,M_\odot$, and supermassive BHs, with masses $\sim 10^6 - 10^9\,M_\odot$ (see, e.g., Fryer & Kalogera 2001; Peterson 2003; Tegmark 2002). However, over the last few years, evidence has been mounting for the existence of *intermediate-mass* BHs (Miller & Colbert 2004). Although the observations remain controversial a variety of plausible formation scenarios for intermediate-mass BHs (IMBHs) have been proposed (e.g., van der Marel 2003). Primordial formation of massive BHs in the early universe has been discussed for many years (e.g., Carr 1993; Khlopov, Rubin & Sakharov 2002). Later on, when the first very massive metal-free (Pop III) stars form, one naturally expects that, given the lack of significant wind mass loss, these stars may collapse to form IMBH remnants with masses up to $\sim 10^2 - 10^3\,M_\odot$ (e.g., Heger et al. 2003). Some of these IMBHs may be in binaries either formed through captures in dense environments (Wyithe & Loeb 2003) or remaining from primordial Pop III binaries (Belczynski, Bulik & Rudak 2004a). Dynamical formation processes for IMBHs in Pop II and Pop I star clusters have also been the subject of many recent studies. The two most promising scenarios involve runaway collisions and mergers of massive main-sequence stars (Portegies Zwart & McMillan 2002; Gürkan, Freitag, & Rasio 2004) and successive mergers of stellar-mass BH (Miller & Hamilton 2002). In this paper, we focus on the populations of stellar BHs forming out of the most massive stars in Pop II or Pop I young stellar environments.

Stellar BHs form through core collapse of massive stars with masses $\gtrsim 20\,M_\odot$. If N stars form with a standard Kroupa (Kroupa & Weidner 2003) initial mass function (IMF) between $M_{\rm min} = 0.08\,M_\odot$ and $M_{\rm max} = 150\,M_\odot$, we expect $N_{\rm BH} \simeq 5\times 10^{-4}\,N$ black holes to have formed after $\sim 10^7$ yr, when all stars massive enough to produce a BH have evolved. The goal of this paper is to characterize this initial population of BHs. For a population of *single stars*, this is merely a question of characterizing the metallicity-dependent relation between progenitor mass and final BH mass (Fryer & Kalogera 2001; Heger et al. 2003). However, most stars, and, especially, most massive stars are expected to form in binary systems (Duquennoy & Mayor 1991). The BH formation processes can be affected significantly by the evolution of the progenitor star in a binary, especially if the initial orbital separation is $\lesssim 500\,R_\odot$ and the star can overflow its Roche lobe as it evolves. In addition, many BHs will retain binary companions, which can drastically affect their later evolution, their detectability as X-ray or gravitational-wave sources, and the way they interact with their environment.

The study we present in this paper is based on a population synthesis approach, in which a large number of single and binary stars are evolved according to parametrized evolutionary prescriptions. Stellar evolution is followed starting from a population of zero-age main-sequence (ZAMS) stars with specified metallicity. Given enough time the stars evolve to form remnants, either white dwarfs (not relevant for the massive stars considered here), neutron stars, or BHs. Both observations and more detailed theoretical calculations are used to constrain and parametrize the uncertain stages of evolution (e.g., supernova explosions and common envelope phases). A number of population synthesis codes of varying levels of sophistication are currently being used to study many astrophysical problems (e.g., Fryer, Woosley, & Hartmann 1999; Nelemans, Yungelson & Portegies-Zwart 2001; Hurley, Tout & Pols 2002; Pfahl, Rappa-

port, & Podsiadlowski 2003; Belczynski, Kalogera & Bulik 2002, hereinafter BKB02). Here we use the most recent version of the `StarTrack` population synthesis code (BKB02; Belczynski et al. 2004b) to study BH formation in young metal-rich (Pop I) and metal-poor (Pop II) populations. This work is complementary to the previous study of the oldest binary BHs, descendants of metal-free Pop III stars, by Belczynski et al. (2004a).

Our results can be applied directly to the modeling of young starburst populations, with ages $\sim 10^7 - 10^8$ yr. For those systems, we have derived complete synthetic sample catalogues of all BHs, single and in binaries, that have evolved from the initial burst of star formation. Our results can also be applied to the modeling of young star clusters (such as the super star clusters so prevalent in starbursts; see, e.g., de Grijs et al. 2003), although we do not take into account the effects of dynamical interactions in dense cluster cores (cf. Gürkan, Freitag & Rasio 2003; Ivanova et al. 2004).

Characterizing the properties of a primordial BH population is also very important for many theoretical studies of old star clusters. Indeed many of these studies attempt to bypass the first $\sim 10^7$yr of massive star evolution and use initial conditions that already contain BHs. For example, N-body simulations of globular clusters containing primordial BHs have been performed starting with a small number of identical single BHs of mass $10\,M_\odot$ (e.g., Fregeau et al. 2002; Portegies Zwart & McMillan 2000). One goal of our work is to provide more realistic initial conditions for those studies. The further dynamical evolution of BHs in dense star clusters could play a key role in many problems of great current interest, such as understanding the formation of IMBHs and ultraluminous X-ray sources (Miller & Hamilton 2002) and predicting the merger rate of BH binaries detectable by gravitational-wave detectors (Portegies Zwart & McMillan 2000).

Our paper is organized as follows. In § 2 we describe the evolutionary model used in the population synthesis calculations, including details about BH formation. In § 3 we present the results of our calculations. First we present the results for our reference model, then we follow with the description of a number of alternative models. Finally, in § 4 we summarize our main results.

2. MODEL DESCRIPTION AND ASSUMPTIONS

2.1. *Population Synthesis Code*

Our calculations are based on a population synthesis method. The `StarTrack` code (BKB02) has recently undergone major revisions and updates (Belczynski et al. 2004b). These include: a detailed treatment of tidal dissipation effects; individual treatments of various Roche lobe overflow (RLOF) phases; full numerical orbit evolution with angular momentum losses due to magnetic braking, gravitational radiation (GR), mass transfer/loss, and tidal interactions, and incorporating the stabilizing influence of optically thick winds.

All stars are evolved based on the metallicity-dependent models of Hurley, Pols, & Tout (2000), with the improvements described in BKB02. Each star, either a single or a binary component, is initiated on ZAMS, and its evolution is followed from ZAMS through a sequence of evolutionary phases: Main Sequence (MS), Hertzsprung Gap (HG), Red Giant Branch (RG), Core Helium Burning (CHeB), Asymptotic Giant Branch (AGB), and for stars stripped off their hydrogen-rich layers Helium phases (He). The nuclear evolution of a star ends at the formation of a stellar remnant: a white dwarf (WD), a neutron star (NS) or a BH.

We adopt parameters corresponding to the standard model of BKB02 (see § 2 in BKB02) incorporating the latest natal kick velocity distribution of Arzoumanian, Chernoff & Cordes (2002), and limiting the accretion rate onto the NS and the BH at the maximum Eddington limit with the rest of the transferred material lost with specific orbital angular momentum of the accretor during the dynamically stable RLOF events, but allowing for hyper-critical accretion during common envelope (CE) phases. During dynamically stable phases with non-compact accretors, we allow for non-conservative evolution, with half of the transferred mass lost with the specific angular momentum equal to $2\pi j A^2/P$, where P is orbital period, A binary separation, and we choose the scaling parameter $j = 1$ for our calculations (Podsiadlowski, Joss & Hsu 1992). In addition to dynamically unstable RLOF events we also allow for evolution into the CE phase in cases where the trapping radius exceeds the Roche lobe radius of the accretor (e.g., King & Begelman 1999; Ivanova et al. 2003). Phases preceding CE are driven by angular momentum losses (as described above), while the inspiral during CE is treated in the standard manner through a prescribed energy efficiency (with $\alpha_{\rm ce} \times \lambda = 1$ in our standard model; for details see BKB02).

2.2. *Black Hole Formation*

BHs are formed out of the most massive stars. Using the stellar models of Hurley et al. (2000) and Woosley (1986) we estimate the time of core collapse of the massive star. At that time we know the mass of the core (both CO and FeNi core) and the envelope. For intermediate-mass stars ($\sim 20 - 30$ M$_\odot$ for low metallicity models) the FeNi core is collapsed to form a hot proto-NS or a low-mass BH, and we use the work of Fryer (1999) and Fryer & Kalogera (2001) to decide how much fall back is expected in a given case (based on the mass of the CO core). Fall-back material is accreted onto the central object, increasing its mass, while the rest is assumed to be ejected in the supernova (SN) explosion. For the highest masses ($\gtrsim 30$ M$_\odot$ for low metallicity models), the entire star goes into collapse, forming the BH directly, with no accompanying SN explosion. The regime for direct BH formation may be easily seen from Figure 1 (pre-collapse mass equal to the remnant mass).

The large observed velocities of radio pulsars imply significant asymmetries in SN explosions. Although the underlying mechanism is not yet understood, it is generally accepted that NS can receive substantial kicks at birth ($\sim 100 - 1000\,{\rm km\,s^{-1}}$). Here we adopt the latest NS kick velocity distribution of Arzoumanian et al. (2002). Most recent observations (e.g., Mirabel & Rodrigues 2003) suggest that BHs may be formed either with an accompanying kick (for smaller mass stellar BHs) or without one (for the most massive stellar BHs). This folds naturally into our prescription for BH formation. For low-mass, fall-back BHs, we expect somewhat attenuated SN explosions, and we assume that the kick is smaller as well: its magnitude is assumed to be inversely proportional to

the mass of fall-back material. For direct BH formation (so called *silent* collapse) there is no explosion, and we therefore assume no asymmetry and no natal kick.

In Figure 1 we show the initial-to-final mass relation for single stars for 3 representative metallicities (Z =0.02, 0.001, 0.0001). Remnants of various types are shown with different symbols. We also plot the instantaneous mass of the star just prior to the formation of the compact remnant.

The top panel of Figure 1 shows the initial-to-final mass relation for solar metallicity ($Z = 0.02$), the case described and discussed in detail in BKB02: BHs are formed from stars more massive than about $20 M_{\odot}$, with a maximum BH mass of $11 M_{\odot}$. There is a general rise of BH mass with increasing progenitor mass. However, since the wind mass-loss rate increases with the mass of the star as well (depleting the mass reservoir for BH formation) the initial-to-final mass relation flattens out for higher progenitor masses. There are two distinctive dips, followed by the subsequent flattening of the relation. The first (around $25\,M_{\odot}$), less pronounced dip corresponds to the point at which single stars are depleted of their H-rich envelopes, entering the Wolf-Rayet stage with enhanced wind mass-loss rates (Hamann & Koesterke 1998). Higher mass-loss rates reduce the mass of the star and its core, eventually leading to the formation of lower-mass remnants. The second dip (around $50\,M_{\odot}$), corresponds to the point where stars reach luminosities high enough to initiate the Luminous Blue Variable (LBV) phase, characterized by extremely high wind mass-loss rates (Hurley et al. 2000), and a sudden decrease of BH masses.

The middle and bottom panels of Figure 1 show the initial-to-final mass relations for lower metallicities ($Z = 0.001$ and $Z = 0.0001$, respectively). In each case the relation differs significantly from that obtained for higher (solar) metallicity. In particular, there is an increase of the maximum BH mass (to $\sim 27 M_{\odot}$ for $Z = 0.001 - 0.0001$), and the shape of the relation is also altered. Most of these changes can be attributed to the dependence of the wind mass-loss rates on metallicity. Here we have adopted wind mass-loss prescriptions with square-root dependence on metallicity ($\propto \sqrt{Z/Z_{\odot}}$), operating however only during specific evolutionary phases (for details see Hurley et al. 2000). The obvious consequence of smaller mass loss rates for lower metallicity is the increase of the stellar mass just prior to the formation of the remnant, leading directly to higher BH masses. In addition, the smaller mass-loss rates imply that the stars encounter the LBV dip at a lower mass ($\sim 33 M_{\odot}$ for $Z = 0.001 - 0.0001$) as they evolve to higher luminosities. The opposite is true for the Wolf-Rayet dip, as now only the stars with much higher mass lose enough material to become naked helium stars ($\sim 38 M_{\odot}$ for $Z = 0.001 - 0.0001$). Note the interesting repositioning of the two dips: for solar metallicity the dip at high mass corresponds to the LBV phase, while for lower metallicity ($Z = 0.001 - 0.0001$) it corresponds to the start of the Wolf-Rayet phase.

Figure 1 also allows us to see the change in relative numbers of BHs formed through fall back or direct progenitor collapse. This is important for survival of the BHs in binary systems, since for fall-back BHs, which receive natal kicks, the systems hosting BH progenitors may be disrupted by SN explosions. For solar metallicity many BHs are formed with kicks through fall back, which occurs for single stars with initial masses in the range $20 - 42\,M_{\odot}$ and $48 - 70\,M_{\odot}$. For $Z = 0.001$, BHs receive a kick in the narrower ranges $18 - 25\,M_{\odot}$ and $39 - 54\,M_{\odot}$. For an even lower metallicity of $Z = 0.0001$, only BHs formed from stars in the mass range $18 - 24\,M_{\odot}$ receive a kick, while all others form silently.

3. RESULTS

3.1. *Standard Reference Model*

Our reference model starts with 10^6 binaries and 10^6 single stars (initial binary fraction $f_{\rm bi} = 50\%$). The initial masses of single stars and binary system primaries (more massive) are chosen from a standard initial mass function (IMF) with slope -2.35 between $4\,M_{\odot}$ and the maximum mass $M_{\rm max}$, characteristic of young clusters (see Kroupa & Weidner 2003 for detailed discussion). We adopt $M_{\rm max} = 150\,M_{\odot}$ for the reference model calculation. The masses of secondary stars in binary systems are sampled from a mass ratio (q, secondary/primary) distribution assumed to be constant between 0 and 1 for our standard model calculation (but values below the hydrogen burning limit at 0.08 $M_{\odot}$ are rejected). The distribution of initial binary separations is assumed to be constant in logarithm between the minimum (such that binary components at ZAMS are not in contact) and $10^5\,R_{\odot}$, while for eccentricities we assume a thermal distribution. In our standard model all stars have metallicity $Z = 0.001$.

Here we define a BH as a compact object with a mass exceeding the maximum NS mass $M_{\rm max,NS} = 3\,M_{\odot}$ (this value will be changed later). We examine the BHs at five different epochs: 8.7 Myr (corresponding to a turnoff mass $M_{\rm to} = 25$ $M_{\odot}$), 11.0 Myr ($M_{\rm to} = 20$ $M_{\odot}$), 15.8 Myr ($M_{\rm to} = 15$ $M_{\odot}$), 41.7 Myr ($M_{\rm to} = 8$ $M_{\odot}$) and 103.8 Myr ($M_{\rm to} = 5$ $M_{\odot}$). The binaries can produce both BHs in binaries and single BHs. For the BHs still in binaries we list the numbers formed in various binary configurations.

Single BHs originating from binaries are formed through several different channels. First, the binary may be disrupted in a SN because of mass loss and a possible nascent kick. In this case the evolution of the two components is followed as two single stars. Single BHs formed this way will be listed explicitly under the category "Single: binary disruption". Binary components may also merge following close interactions (e.g., CE evolution, Darwin instability) forming a single object, which may later evolve and leave behind a single BH (denoted by the category "Single: binary merger"). The merger product is assigned a new mass, either the total component masses for mergers involving compact remnants or MS stars or their core masses in cases involving giant-like stars (with the envelopes assumed lost during the merger process). If one component is already a BH, we assume that the outcome of the merger is still a BH (formed instantaneously, with a new higher mass). In all other cases, we assume the formation of a new ZAMS star (i.e., "full rejuvenation") and we proceed to evolve the new single star. If the merger product is massive enough a (single) BH may form. Since all merging binary components are already evolved, the evolution leading to the

formation of a BH in this case may in reality be somewhat shorter, and thus our predicted numbers for this category are only lower limits. Most of the merger products massive enough to produce BHs are found to have come from pairs of massive HG-MS, He-MS, and MS-MS systems.

In Table 1 we list the numbers of BHs found both as single objects and as members of binary systems. Binary BHs are most frequently found either in BH–MS or BH–BH systems. Shortly after the initial starburst, MS companions naturally dominate (they are the most probable BH companions at early times). However, as the age increases these massive MS companions themselves evolve, collapse to BHs and some eventually form BH–BH systems (dominating at later times). The second longest lived phase in massive star evolution (after the MS) corresponds to core helium burning. We note a similar trend for BH–CHeB as for BH–MS binaries. Although naturally less numerous overall, the number of BH–CHeB binaries peaks as soon as these systems appear but then tends to decrease with time. As the less massive progenitors end their lives and start forming remnants, we observe increasing numbers of BH–NS and later BH–WD systems.

There is an overall decrease in the number of binary BHs with time. This can be understood as follows. Most massive stars have finished their evolution and formed BHs at early times ($\lesssim 10$ Myr). Many of the BH binaries with unevolved MS companions either merge in RLOF events or are disrupted when the secondary star undergoes a SN explosion. At later times, some of the tightest binaries may also merge due to orbital decay driven by GR emission. The opposite trend—increase with time—is seen in the total number of single BHs. After the first ~ 10 Myr most of the single BH progenitors have finished their evolution and have formed BHs; therefore the later increase is connected to binary evolution. The binary mergers and disrupted components continue adding to the single BH population at later times. For an initial 50% binary fraction we predict that single BHs eventually dominate by about an order of magnitude over BHs found in binaries.

There is an interesting direct relationship between the relative numbers of binary and single BHs for any specific starburst and its initial (primordial) binary fraction. Etc. Let us define the ratio of binary to single BHs (as a function of the initial binary fraction $f_{\rm bi}$) as $R(f_{\rm bi}) = (100\%\ N_{\rm bin})/N_{\rm sin}$, where $N_{\rm bin}$ and $N_{\rm sin}$ denote the total number of BHs found in binaries and as single objects, respectively. Obviously, this ratio is also a function of age, but, for definiteness, let us pick a specific age of $t = 11\,$Myr. For an initial population consisting *entirely* of binaries ($f_{\rm bi} = 100\%$ from Table 1 we can read that the total number of binary BHs is 27729 while the number of single BH is 64271 (all from binary disruptions and mergers), so the ratio $R(f_{\rm bi} = 100\%) = 0.37$. This is obviously an upper limit. Any contribution from single stars in the initial population will lower this value.

3.2. *Parameter Study and Normalization*

To assess the effects of various model assumptions on BH formation, we repeat our calculations for a number of different models, each differing from our standard reference model in the value of one parameter or one assumption. The specific models we chose are described in Table 2.

Normalization: In addition to a brief description of each model, Table 2 also lists for each simulation the total initial mass of single and binary stars. All stars are assumed to form in an instantaneous burst of star formation. Stars can form from the hydrogen burning limit up to the maximum mass $M_{\rm max}$ characterizing a given system. We adopt the three-component, power-law IMF of Kroupa, Tout, & Gilmore (1993) with slope $\alpha_1 = -1.3$ within the initial mass range $0.08 - 0.5\ {\rm M}_\odot$, $\alpha_2 = -2.2$ for stars within $0.5 - 1.0\ {\rm M}_\odot$, and $\alpha_3 = -2.35$ within $1.0\,M_\odot - M_{\rm max}$. This IMF is easily integrated to find the total mass contained in single and binary stars for any adopted α_1, α_2 values. The particular choice of low-mass end slope of the IMF (α_1, α_2) usually (with the exception of Model B) does not change our results. Low-mass stars do not contribute to the BH populations. However, as most of the initial stellar mass is contained in low-mass stars, a small change in the IMF slope at the low-mass end can significantly change the normalization. Similarly, our results can easily be generalized to other primordial binary fractions ($f_{\rm bi}$) by simply weighing differently the results obtained for single stars and for binaries.

Summary of results: In Table 3 we summarize the state of each simulation at 11 Myr ($M_{\rm to} = 20\ {\rm M}_\odot$) for the models presented in Table 2. In the following, we describe in more detail how the changes made in each model affect the various BH populations.

In Model B we create the binary by independently (1) drawing the primary from $4 - 150 M_\odot$ according to an IMF exponent -2.35 and (2) drawing the secondary from $0.08 - 150 M_\odot$ via the Kroupa broken power-law IMF. This initialization process results in the ratio q of component masses peaked at low q values. For this model, almost all BHs in binaries are found with MS companions. In addition, relative to the reference model, fewer single BHs are produced from disrupted binaries. Since the initial mass ratio is on average smaller in Model B, massive stars, the progenitors of BHs, are formed preferentially with low-mass MS companions. If a BH progenitor does not destroy the binary, then the low mass companion remains for a long time on MS (large number of BH–MS systems) and it does not initiate either RLOF nor explode as SN (small numbers of single BHs). In contrast to the standard model, there are almost no BH–BH systems, as they originate typically from binary progenitors with relatively high mass ratios that are almost absent in Model B.

For Model C1 we use small metallicity $Z = 0.0001$ (characteristic of old Pop II stars metallicity) while for Model C2 we choose high (solar) metallicity of $Z = 0.02$. We find that the total number of BHs formed can vary strongly with the initial chemical abundance. While single BHs are not greatly affected, the population of binary BHs changes drastically with metallicity. With increasing metallicity the evolution of the star is altered; most notably, the stellar wind mass loss rate increases, causing the star's mass to drop more rapidly. Eventually, some stars either form lower mass BHs or instead of forming BHs they end up as NSs. Also higher wind mass loss rates (Model C2) and their associated angular momentum losses leave binaries wider, and therefore

i) easier to disrupt (see the increase of single BHs from binary disruption), *ii)* making component interactions harder (smaller chance of RLOF; see the smaller merger BH number). To summarize, then, the BH population formed from binary stars depends sensitively on the characteristic metallicity of the primordial population.

In Model D we decrease the CE efficiency to 0.1, which means that only 10% of binary orbital energy may be used for envelope ejection. This leads to either merger of binary components in CE phase, or results in a much tighter orbit of post-CE binary, if it survives. There is no significant change in the number of BHs in Model D as compared to the reference model. Only the close binaries with rather extreme mass ratios undergo a dynamically unstable RLOF, and thus their evolution may be altered in Model D. This obviously depletes number of BH–MS stars (as they tend to have rather small mass ratios, otherwise a MS star would have already evolved to a BH), while leaves the number of BH–BH systems unchanged (formed at early times out of comparable mass binary components). Further orbital shrinkage during the dynamically unstable RLOF events obviously increases the number of binary mergers (especially in the second RLOF episode), but the merger products do not have enough time to form BHs after 11 Myrs. [1] Finally the binaries which evolved through one or two CE events are tighter and are harder to disrupt in SN explosions (explaining the slight decrease in the number of BHs from binary disruptions).

In Model E, we apply for all BHs, independent of their mass and formation scenario, full nascent kicks following the distribution of Arzoumanian et al. (2002). By contrast, in our standard model, we either have used smaller kicks or no kicks at all for BH formation. Therefore, we expect (and observe) a drastic decrease in number of BHs formed in binary systems, since full kicks disrupt all wide and also many close binaries. Further, since systems that would otherwise be binary BHs are disrupted, we produce many more single BHs than in our reference model. Although the nascent kicks play an important role in the modeling of BH binary populations, we note that the most massive BHs almost certainly form silently (Mirabel & Rodrigues 2003), without nascent kicks, so the results of Model E should be treated as an extreme case.

In Model F, for high-mass stars (potential BH progenitors), we use a steeper IMF exponent ($\alpha_3 = -2.7$), similar to the one observed in field populations. As expected, all the numbers for BHs found in binaries and as single objects are decreased. Although we do not expect the initial starburst IMF to be as steep as the one observed in the field (Kroupa & Weidner 2003), it is worth noting the factor of 2 decrease in BH numbers for this choice.

Since smaller, less massive clusters form stars only up to a smaller maximum mass, in Models G1 and G2, we decrease $M_{\rm max}$ to 50 and 100 $M_\odot$, respectively. A decrease in the maximum stellar mass in a given simulation shifts more stars to lower mass, depleting the number of potential BH progenitors. Therefore there is a general decrease of BH numbers found in Models G. Since more BH progenitors are removed from initial population in Model G1, it shows the largest change as compared to the standard model calculation. However, due to a steep IMF for massive BH progenitors, the high mass end missing in Models G1 and G2 does not contain many stars and the change is not large.

In Model H we show results for a lowered maximum mass for NS formation, which may be as low as $1.8-2.3$ $M_\odot$ (see, e.g., Akmal, Pandharipande, & Ravenhall 1998). In this model we adopt $M_{\rm max,NS} = 2M_\odot$, and all compact objects over that mass are assumed to be BHs. As expected, this model has slightly more single and binary BHs. Clearly the maximum NS mass is not significant compared to other model uncertainties.

Finally, under "Model I" (which is not really a different model), we give the numbers of BHs with mass greater than $10M_\odot$ found in our reference model. Since most of the single stars and non-interacting binary components form BHs with $M \gtrsim 10$ $M_\odot$ (see Fig. 1), there is only a slight decrease in BH numbers.

In Table 4 we present the subpopulations of single and binary BHs at 103.8 Myr ($M_{\rm to} = 5$ $M_\odot$). The trends are very similar to these observed at the earlier epoch (Table 3), however, with the increased contribution of remnant BH binaries (BH–NS and BH–WD).

3.3. *Orbital Periods of Black Hole Binaries*

Period distribution for the standard model: In Figure 2 we plot the distribution of orbital periods of BH binaries for our standard model calculation at $t = 11$ Myrs after starburst. This figure also shows the contributions from the BH–MS and BH–BH subpopulations.

Orbital periods of binaries hosting BHs are found in a very wide range $P_{\rm orb} \sim 0.1-10^6$ days. The distribution is characterized by two distinctive peaks, smaller at $P_{\rm orb} \sim 10$ days, and larger at $P_{\rm orb} \sim 10^5$ days, with the underpopulated region ($P_{\rm orb} \sim 10^3$ days) in between. The clear distinction between short and long period binaries is caused by progenitor system RLOF history or lack of thereof. There is a bifurcation period at $P_{\rm bur} \sim 10^3$ days: below which systems go at least through one RLOF interaction leading most frequently to the orbital shrinkage, while the wider systems never interact, but only lose material in stellar winds, and their orbits expand. The specific value of $P_{\rm bur}$ is different for each binary, and depends on the maximum radii the components may reach in their evolution (set by initial mass and metallicity). If at any moment of the binary evolution radius of either component increases over its Roche lobe radius (set by the period and mass ratio) then RLOF starts. Therefore, the $P_{\rm bur}$ is a function of a number of parameters describing the binary and its components and it depends also on the orbit evolution (e.g., tidal interactions), and it is found within a range: $P_{\rm bur} \sim 100-10^4$ days for binary BH progenitors. Since the tighter binaries evolve through one or more RLOF interactions, many of them merge, and single objects are formed, causing the depletion of the short-period binary BH population (smaller peak). Although wide binaries avoid mergers, they are much more prone to the disruption in SN explosions. However, since most of BHs are formed silently or with rather small kicks, the depletion is not large, and the peak at long periods is substantially higher than for tighter binaries.

The BH–BH binaries evolve only through GR. Their

[1] Note that at later epoch the number of binary mergers has increased by factor of ~ 3 (see Table 4).

orbits decay slowly, and for the tightest binaries the two components can merge and produce a single BH (within a Hubble time).

Systems containing a non-remnant companion (e.g., BH–MS, BH–CHeB), given enough time, will populate other BH subpopulations. In particular, if the companion is massive enough to form a second BH in the system, and the binary survives potential interactions and SN explosion, a BH–BH binary will be formed. It is worth noting that the majority of the binaries are quite "soft," with long periods $P_{\rm orb} \gtrsim 100$ days, so that, if placed in a dense stellar environment (e.g., a globular cluster) they will be easily disrupted, further enhancing the single BH population. On the other hand, a smaller but significant number of binaries are hard and, through dynamical interactions with other stars, may even become harder (evolve to shorter periods). The overall shape of the distribution remains mostly unchanged at different times (listed in Table 1). However, as discussed in § 3.2, the contribution of the BH–BH binaries increases, while the BH–MS systems are relatively less frequent at the later times.

Dependence of period distribution on model assumptions: In Figure 3 we present period distributions of BH binaries for all our alternative evolutionary models.

In most cases (e.g. Models B, C1, D, F, G1, G2 and H), the general two-peaked shape of our reference model distribution is preserved. For some of these models position and/or relative hight of the two peaks may change slightly, for reasons that can be easily explained in terms of the different model assumptions. For example in Model D, we find that the number of tight binaries in comparison with long-period systems is much smaller than for the reference model. Moreover, the gap between the two peaks is more pronounced and wider than for the reference model. Model D simulations used smaller CE efficiency, affecting tight interacting binaries by shifting them to smaller orbital periods (wider gap) or leading to component merger (smaller peak at low periods).

For a few models, the changes in the distribution are much more pronounced. In Models C2 (high metallicity) and I (high mass BHs only) the distribution is peaked at large orbital periods, while the short period BH binaries, are relatively very infrequent. For example, the Model I evolution (which favors only the highest mass progenitors) leads to a selection and survival of only the widest binaries. If the high mass stars, progenitors of the most massive BHs, are placed on the tight orbits, they merge in the first RLOF interaction, and the formation of the tight BH system is aborted. In contrast with previous two, in Model E, we find that almost all of the BH binaries have short orbital periods. With full kicks applied to all BHs, almost all wide systems are disrupted.

3.4. *Black Hole Masses*

Mass distribution for the standard model: In Figure 4 we plot the mass distribution of the entire BH population formed in our standard Model A. Additionally, we plot separately the single and binary BH subpopulations. The distribution shows three well defined peaks, first at $M_{\rm BH} \sim 6-8$ M$_\odot$, second at $M_{\rm BH} \sim 10-16$ M$_\odot$, and third at $M_{\rm BH} \sim 22-26$ M$_\odot$, and then it steeply falls off with the increasing BH mass. The distribution may be divided into two major contributions, one from the population of single BHs, and the other from BHs in binaries. We see that single BHs dominate the population (see also § 3.2) and basically set the shape of the overall mass distribution. A majority of the single BHs originate either from single star progenitors or from disruptions of wide (non-interacting) binary stars in SN explosions. Therefore, the shape of distribution for single BHs is mainly determined by a combination of the initial-to-final mass relation for single BHs (Fig. 1) with the IMF. And, in fact, in Figure 1 (middle panel) we can see the pile up of BH remnants corresponding to the three peaks in the BH mass distribution of Figure 4. Stars over ~ 50 M$_\odot$ form $10-16$ M$_\odot$ BHs corresponding to the second, the largest, peak in Figure 4. Stars with initial masses of $25-35$ M$_\odot$ form ~ 25 M$_\odot$ BHs, providing a majority of the third peak in the BH mass distribution. Finally, the stars with initial masses of $40-50$ M$_\odot$ tend to form BHs with masses of ~ 7 M$_\odot$, the first peak of the Figure 4 distribution. The initial-to-final mass relation leading directly to the shape of the BH mass distribution is described in detail in § 3.1. The binary evolution may increase or decrease the mass reservoir for BH formation through RLOF interactions between system components. However, with one or two exceptions, the overall shape of the mass distribution for single and binary BHs is rather similar. Specifically, the most apparent change is that for binary BHs the first narrow peak for BH masses of $6-8$ M$_\odot$ is missing. This peak for single BHs comes from the turnover in the initial-to-final mass relation, resulting in a pile up of BHs in this specific mass range. This characteristic feature of the initial-to-final mass relation corresponds to a very sharp transition in single star evolution, from H-rich to naked helium stars, which is caused by wind mass loss and the effective envelope removal for single stars above a certain initial mass. Since, for binary stars, removal of the envelope is allowed not only through stellar winds but also through RLOF interactions, it is allowed for the entire mass range, and therefore there is no sharp transition between evolution of H-rich and helium reach stars, and the aforementioned peak disappears.

One more important effect of binary evolution on BH final mass is illustrated in Figure 5, where we show single BHs up to the highest formed BH mass. Single BHs form either from single progenitors, from components of disrupted binaries, or through binary mergers. Clearly we can see that single star progenitors form BHs only up to ~ 30 M$_\odot$ (as expected from Fig. 1). Slightly higher BH masses (~ 40 M$_\odot$) are obtained through binary disruption, as some of the progenitors may have been rejuvenated in RLOF event to a higher mass in the preceding binary evolution. All of the most massive BHs, up to ~ 80 M$_\odot$, are formed through binary mergers. Most mergers are formed out of HG–MS pairs, due to the very rapid expansion in the Hertzsprung Gap, leading very often to dynamically unstable RLOF (in which case we always assume a merger; see Ivanova & Taam 2004). In case of such a merger, the final mass of the newly formed single star is the sum of the MS star mass and the core mass of the HG star (the envelope of the HG star, containing $\gtrsim 50\%$ of the entire star mass, is assumed to be lost in the merger process). Since we allow for significant mass loss in the merger process, the final merger remnant mass may be underestimated. Had we assumed that all

mass in the system remains after merger, some of BHs produced through this channel would have even larger masses, $\gtrsim$ 100 $M_\odot$. These objects have high enough masses to be classified observationally as "intermediate-mass" BHs. However, it is important to note that they are formed through ordinary binary star evolution, without the need for additional dynamical interaction processes.

Effects of model assumptions on mass distribution: In Figures 6 and 7 we present the BH mass distributions for all the models in our parameter study. The overall distribution for the entire BH population is not greatly affected by different choices of parameter values, with the exception of metallicity (see Fig. 6). This is easily understood, as the highest mass BHs are formed only at the low metallicity (Models C1 and A) and the lightest BHs are formed at the high metallicity (Model C2) as discussed in § 3.1. Single BH masses (Fig. 7) in many models reach very high values around 80 $M_\odot$, and this is a robust result of our calculations for a number of different evolutionary and initial conditions. The highest maximum BH masses are found for lowest metallicity environments, in a larger systems (with high $M_{\rm max}$), and for binaries formed with flat mass ratio distributions, quite independent of other evolutionary parameters. Only in a few models, with high metallicity (C2), uncorrelated initial binary component masses (B), and low $M_{\rm max}$ (G1, G2), does the maximum BH mass stay below ~ 50 $M_\odot$.

GR emission: BH–BH binaries (rather than double NSs), are probably the best candidates for detection by ground-based interferometers (Lipunov, Postnov, & Prokhorov 1997; Bulik & Belczynski 2003). BH–BH systems therefore are an important candidate for present projects to detect astrophysical GR sources (LIGO, VIRGO). The properties of BH–BH binaries at different metallicities formed within much larger stellar systems with continuous star formation (e.g., Galactic disk) were extensively studied previously (Bulik & Belczynski 2003; Bulik, Belczynski & Rudak 2004a; Bulik, Gondek-Rosinska & Belczynski 2004b). We find that the properties of BH–BH binaries in starbursts are not too different from those found in the previous studies. Most of BH–BH systems are characterized by rather equal masses, with a mass ratio distribution peaking at $q \simeq 0.8-1.0$ (for comparison see low-metallicity models of Bulik et al. 2004b). For most models only a small fraction ($\sim$ few per cent; e.g., 2% for Model A) of the BH–BH systems are tight enough to merge within a Hubble time and produce observable GR signals. However, for models which tend to produce tighter BH–BH systems (D, E) the fraction can be significantly higher ($\sim$ 10–20 %).

4. SUMMARY

We have calculated the evolution of the massive stars found in young stellar environments, such as starbursts. The final products of massive star evolution, single and binary BHs, were then studied. All our results were discussed taking into account the many model uncertainties. A number of alternative calculations with varied initial conditions and evolutionary parameters were performed and presented. We also supplied the necessary data to normalize our results to any given total mass of a starburst galaxy or star cluster, with arbitrary choice of initial binary fraction. The calibrated results may then be used as part of initial conditions for realistic N-body simulations of dense stellar clusters that include primordial BHs.

Soon after the initial star formation burst, most BHs are found as single objects, although a significant fraction of BHs are also found in binaries. A number of single BHs are formed as the end product of binary evolution, either through binary disruption following a SN explosion or through a merger following a dynamically unstable RLOF episode. The most common binary BHs are BH–MS and BH–BH systems. The period distribution of binaries containing BHs is usually bimodal, with a majority of systems in the long period peak ($P \sim 10^4 - 10^6$ days). These wide binaries would be "soft" if placed in a dense stellar environment (e.g., a globular cluster) and they would then be disrupted following any strong interaction with another passing star or binary, thereby further enhancing the population of single BHs. The remaining, short-period BH binaries ($P \sim 1-100$ days) would instead undergo hardening and evolve, over many relaxation times, to produce a population of very compact binaries that could eventually merge through GR emission.

The typical BH masses are found to be within the range $7-25$ $M_\odot$, both for single and binary BHs. However, the single BHs formed through binary mergers can reach masses as high as ~ 80 $M_\odot$. Since most mergers are assumed in our models to be accompanied by significant mass loss, BHs formed through binary evolution (without any dynamical interactions) could in principle reach even higher masses, up to ~ 100 $M_\odot$ (in the absence of significant merger-induced mass loss). This result has many important implications. First, some ultra-luminous X-ray sources might be explained by a ~ 100 $M_\odot$ *stellar* BH accreting from a lower-mass companion. This would require the capture of a new companion (most likely through an exchange interaction with another binary), but no dynamics would be involved in the BH formation (cf. Kalogera, King, & Rasio 2004). Second, these most massive stellar BHs may act as seeds for the formation of true IMBHs (with masses $\gtrsim 1000$ $M_\odot$) that could reside at the centers of some dense star clusters (Gebhardt, Rich, & Ho 2002; Gerssen et al. 2002; Miller & Hamilton 2002). Third, a broader mass range for the tightest BH–BH binaries (possibly undergoing further hardening through dynamical interactions in a dense star cluster) will modify predictions for the gravitational-wave signals detectable by laser-interferometer instruments such as LIGO and VIRGO (Flanagan & Hughes 1998).

We thank A. Gürkan, R. O'Shaughnessy and M. Tegmark for useful discussions. FAR acknowledges support from NSF Grants PHY-0133425 and PHY-0245028, and from NASA ATP Grant NAG5-12044, and also thanks the Kavli Institute for Theoretical Physics for hospitality. KB and AS acknowledge support from KBN Grant 5P03D01120.

REFERENCES

Akmal, A., Pandharipande, V. R., & Ravenhall, D. G. 1998, Phys. Rev. C, 58, 1804

Arzoumanian, Z., Chernoff, D. F., & Cordes, J. M. 2002, ApJ, 568, 289

Belczynski, K., Bulik, T., & Rudak, B. 2004a, ApJ Letters, submitted (astro-ph/0403361)
Belczynski, K., Kalogera, V., & Bulik, T. 2002, ApJ, 572, 407 (BKB02)
Belczynski, K., Kalogera, V., Rasio, F.A., & Taam, R. 2004b, in preparation
Bulik, T., & Belczynski, K. 2003, ApJ, 589, L37
Bulik, T., Belczynski, K., & Rudak, B. 2004a, A&A, 415, 407
Bulik, T., Gondek-Rosinska, D., & Belczynski, K. 2004b, MNRAS, submitted [astro-ph/0310544]
Carr, B.J. 1993, in The Renaissance of General Relativity and Cosmology, eds. G. Ellis, A. Lanza, and J. Miller (Cambridge: Cambridge University Press), 258
de Grijs, R., et al. 2003, MNRAS, 342, 259
Duquennoy, A., & Mayor, M. 1991, A&A, 248, 485
Flanagan, E.E., & Hughes, S.A. 1998, PRD, 57, 4535
Fregeau, J.M., Joshi, K.J., Portegies Zwart, S.F., & Rasio, F.A. 2002, ApJ, 570, 171
Fryer, C. L. 1999, ApJ, 522, 413
Fryer, C. L., & Kalogera, V. 2001, ApJ, 554, 548
Fryer, C. L., Woosley, S. E., & Hartmann, D. H. 1999, ApJ, 526, 152
Gebhardt, K., Rich, R.M., & Ho, L.C. 2002, ApJ, 578, L41
Gerssen, J., van der Marel, R.P., Gebhardt, K., Guhathakurta, P., Peterson, R.C., & Pryor, C. 2002, AJ, 124, 3270
Gürkan, M.A., Freitag, M., & Rasio, F.A. 2004, ApJ, 604, 632
Hamann, W.R., & Koesterke, L. 1998, A&A, 335, 1003
Heger, A., Fryer, C.L., Woosley, S.E., Langer, N., & Hartmann, D.H. 2003, ApJ, 591, 288
Hurley, J. R., Pols, O. R., & Tout, C. A. 2000, MNRAS, 315, 543
Hurley, J. R., Tout, C. A., & Pols, O. R. 2002, MNRAS, 329, 827
Ivanova, N., Belczynski, K., Kalogera, V., Taam, R. E., & Rasio, F.A. 2003, ApJ, 592, 475
Ivanova, N., Belczynski, K., Fregeau, J.M., & Rasio, F.A. 2004, ApJLetters, submitted (astro-ph/0312497)
Ivanova, N., & Taam, R. E. 2004, ApJ, 601, 1058
Kalogera, V., King, A.R., & Rasio, F.A. 2004, ApJ, 601, L171
King, A. R., & Begelman, M. C. 1999, ApJ, 519, L169
Khlopov, M.Yu., Rubin, S.G., & Sakharov, A.S. 2002, Gravitation & Cosmology, submitted (astro-ph/0202505)
Kroupa, P., Tout, C.A., & Gilmore, G. 1993, MNRAS, 262, 545
Kroupa, P., & Weidner, C. 2003, ApJ, accepted (astro-ph/0308356)
Lipunov, V.M., Postnov, K.A., & Prokhorov, M.E. 1997, NewA, 2, 43
Miller, M.C., & Colbert, E.J.M. 2004, Int. J. Mod. Phys. D, 13, 1
Miller, M.C., & Hamilton, D.P. 2002, MNRAS, 330, 232
Mirabel, I.F., & Rodrigues, I. 2003, Science, 300, 1119
Nelemans, G., Yungelson, L.R., & Portegies Zwart, S.F. 2001, A&A, 375, 890
Peterson, B.M. 2003, in Active Galactic Nuclei: from Central Engine to Host Galaxy, eds. S. Collin, F. Combes and I. Shlosman, (ASP Conference Series, Vol. 290), 43
Pfahl, E., Rappaport, S., & Podsiadlowski, P. 2003, ApJ, 597, 1036
Podsiadlowski, P., Joss, P.C., & Hsu, J.J.L. 1992, ApJ, 391, 246
Portegies Zwart, S.F., & McMillan, S.L.W. 2000, ApJ, 528, L17
Portegies Zwart, S.F., & McMillan, S.L.W. 2002, ApJ, 576, 899
Tegmark, M. 2002, Science, 296, 1427
van der Marel, R.P. 2004, to appear in Carnegie Observatories Astrophysics Series, Vol. 1: Coevolution of Black Holes and Galaxies, ed. L. C. Ho (Cambridge: Cambridge Univ. Press) [astro-ph/0302101]
Wyithe, J.S.B., & Loeb, A. 2003, ApJ Letters, submitted (astro-ph/0312080)
Woosley, S.E. 1986, in 'Nucleosynthesis and Chemical Evolution", 16th Saas-Fee Course, eds. B. Hauck et al., Geneva Obs., 1

Table 1. Black Hole Populations – Standard Model

Type[a]	8.7 Myr $M_{\rm to} = 25$ M$_\odot$	11.0 Myr $M_{\rm to} = 20$ M$_\odot$	15.8 Myr $M_{\rm to} = 15$ M$_\odot$	41.7 Myr $M_{\rm to} = 8$ M$_\odot$	103.8 Myr $M_{\rm to} = 5$ M$_\odot$
BH–MS	17315	16207	12215	6571	4004
BH–HG	22	16	14	16	7
BH–RG	0	0	0	1	0
BH–CHeB	1254	1029	675	262	155
BH–AGB	16	13	27	9	16
BH–He	167	102	60	0	0
BH–WD	0	0	0	1	1075
BH–NS	69	364	760	913	880
BH–BH	9261	9998	10022	10010	9996
Total in binaries:	28104	27729	23773	17783	16133
Single: binary disruption	24093	43909	55649	60262	61021
Single: binary merger	10128	20362	33825	65236	66148
Single progenitor	77580	108080	120100	120100	120100
Total single:	111801	172351	209574	245598	247269

[a]Black holes in binary systems are listed according to their companion types: MS—main sequence, HG—Hertzsprung Gap, RG—reg giant, CHeB—core He burning, AGB—asymptotic giant branch, He—helium star, WD—white dwarf, NS—neutron star, BH—black hole. Single black holes formed from components of disrupted binaries are listed under “Single: binary disruption.” Single black holes formed from binary merger products are under “Single: binary merger.” Single black holes that are remnants of single stars are listed under “Single progenitor.”

Table 2. Population Synthesis Model Assumptions

Model	Description[a]	Mass [$M_\odot$] in Single Stars	Mass [$M_\odot$] in Binaries
A	standard model described in § 3.1	3.8×10^7	5.9×10^7
B	uncorrelated binary component masses	3.8×10^7	7.6×10^7
C1-2	metallicity $Z = 0.0001, 0.02$	3.8×10^7	5.9×10^7
D	$\alpha_{\rm CE} \times \lambda = 0.1$	3.8×10^7	5.9×10^7
E	full kicks for BHs	3.8×10^7	5.9×10^7
F	steeper IMF: $\alpha_3 = -2.7$	6.0×10^7	9.5×10^7
G1	lower maximum mass: $M_{\rm max} = 50 M_\odot$	3.7×10^7	5.8×10^7
G2	lower maximum mass: $M_{\rm max} = 100 M_\odot$	3.8×10^7	5.9×10^7
H	$M_{\rm max,NS} = 2\,{\rm M}_\odot$	3.8×10^7	5.9×10^7
I[b]	BHs more massive than 10 M$_\odot$	3.8×10^7	5.9×10^7

[a]Details of model assumptions are given in § 3.2 and § 3.3.

[b]Model I is shown only to give the numbers of BHs (formed in the standard Model A) with mass greater than $10 M_\odot$.

Table 3. Very Young Black Hole Populations – Parameter Study[a]

Type	A	B	C1	C2	D	E	F	G1	G2	H	I
Binaries:											
BH–MS	16207	32464	25527	2831	12683	3176	9656	13434	15798	17566	11024
BH–HG	16	1	26	7	25	6	10	17	28	16	10
BH–RG	0	0	0	0	0	0	0	0	0	0	0
BH–CHeB	1029	16	1571	200	967	58	616	776	1032	1047	894
BH–AGB	13	0	20	7	25	0	10	13	20	13	12
BH–He	102	3	204	71	26	76	64	102	116	106	22
BH–WD	0	0	0	0	0	0	0	0	0	0	0
BH–NS	364	2	545	94	99	106	180	305	364	55	0
BH–BH	9998	26	20914	2743	10129	196	4784	3127	7496	10326	7674
Total:	27729	32512	48807	5953	23954	3618	15320	17774	24854	29129	19636
Single:											
binary disruption	43909	18929	21037	38110	34806	79260	25696	35858	42022	47714	10863
binary merger	20362	7402	16790	33809	20084	19830	10552	10837	18692	20793	18030
Single progenitor	108080	108080	109755	122470	108080	108080	63090	83695	102255	108080	87630
Total:	172351	134411	147582	194389	162970	207170	99338	130390	162969	176587	116523

[a]All numbers correspond to an age of 11 Myrs ($M_{\rm to} = 20 M_{\odot}$)

Table 4. Young Black Hole Populations – Parameter Study[a]

Type	A	B	C1	C2	D	E	F	G1	G2	H	I
Binaries:											
BH–MS	4004	31762	5952	888	3052	766	2520	3394	3998	4506	2836
BH–HG	7	2	14	0	11	0	6	5	14	7	5
BH–RG	0	0	0	1	0	0	2	0	0	0	0
BH–CHeB	155	50	238	55	153	2	96	104	164	155	151
BH–AGB	16	3	22	6	18	0	8	16	14	16	15
BH–He	0	0	0	0	0	0	0	0	0	1	0
BH–WD	1075	205	1470	459	1064	10	612	779	966	1087	1033
BH–NS	880	13	1705	160	292	356	512	763	980	610	56
BH–BH	9996	26	20915	2743	9745	202	4790	3130	7494	10434	7674
Total:	16133	32061	30316	4312	14335	1336	8546	8191	1630	16816	11770
Single:											
binary disruption	61021	23660	44889	40146	51089	88394	36806	51708	58766	88195	15167
binary merger	66148	19012	54904	88961	74952	64172	43794	57573	65004	68834	49515
Single progenitor	120100	120100	147065	127835	120100	120100	93080	124755	142765	148465	87630
Total:	247269	162772	246858	256942	246141	272666	173680	234036	266535	305494	152312

[a]All numbers correspond to an age of 103.8 Myrs ($M_{\rm to} = 5 M_\odot$)

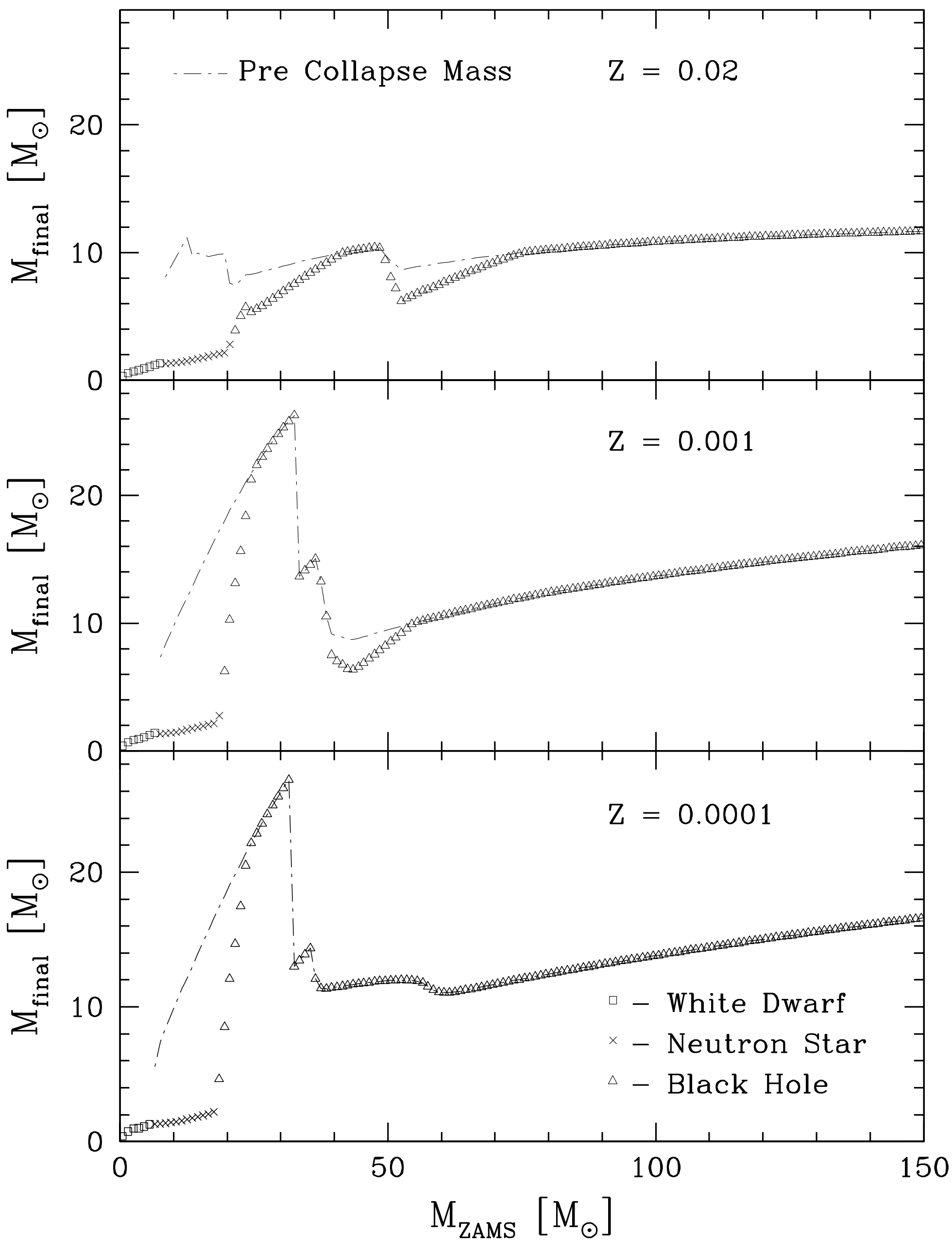

FIG. 1.— Initial-to-final mass relation for different metallicities. Remnants of different type: white dwarfs (WD), neutron stars (NS) and black holes (BH) are marked.

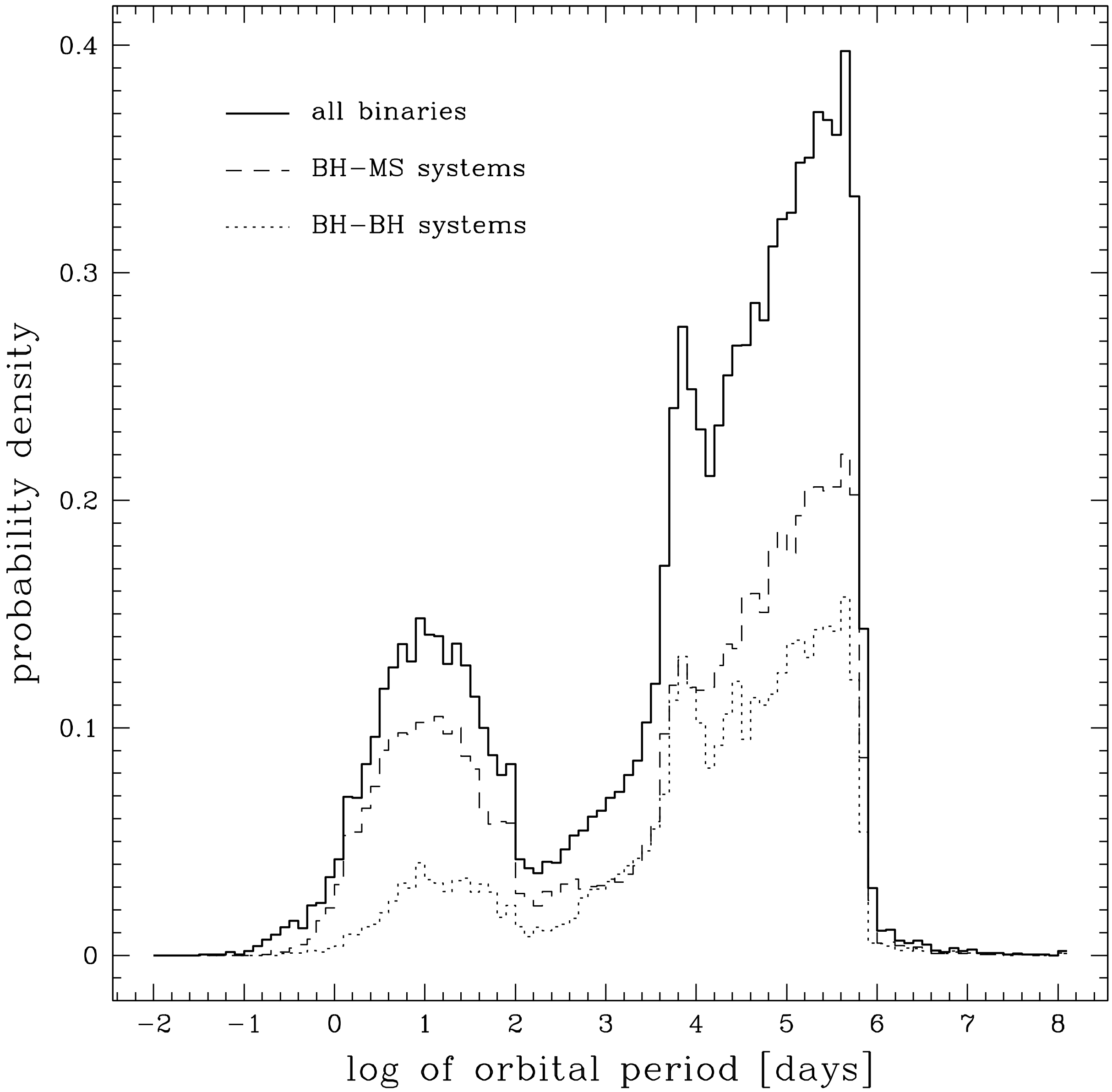

Fig. 2.— Period distribution of BH binaries (solid line) for our standard model after 11 Myr. Two major contributing system types are shown separately: BH–MS binaries (dashed line) and BH–BH binaries (dotted line). Normalized to total number of BHs (single and binaries), binwidth: tenth of decade.

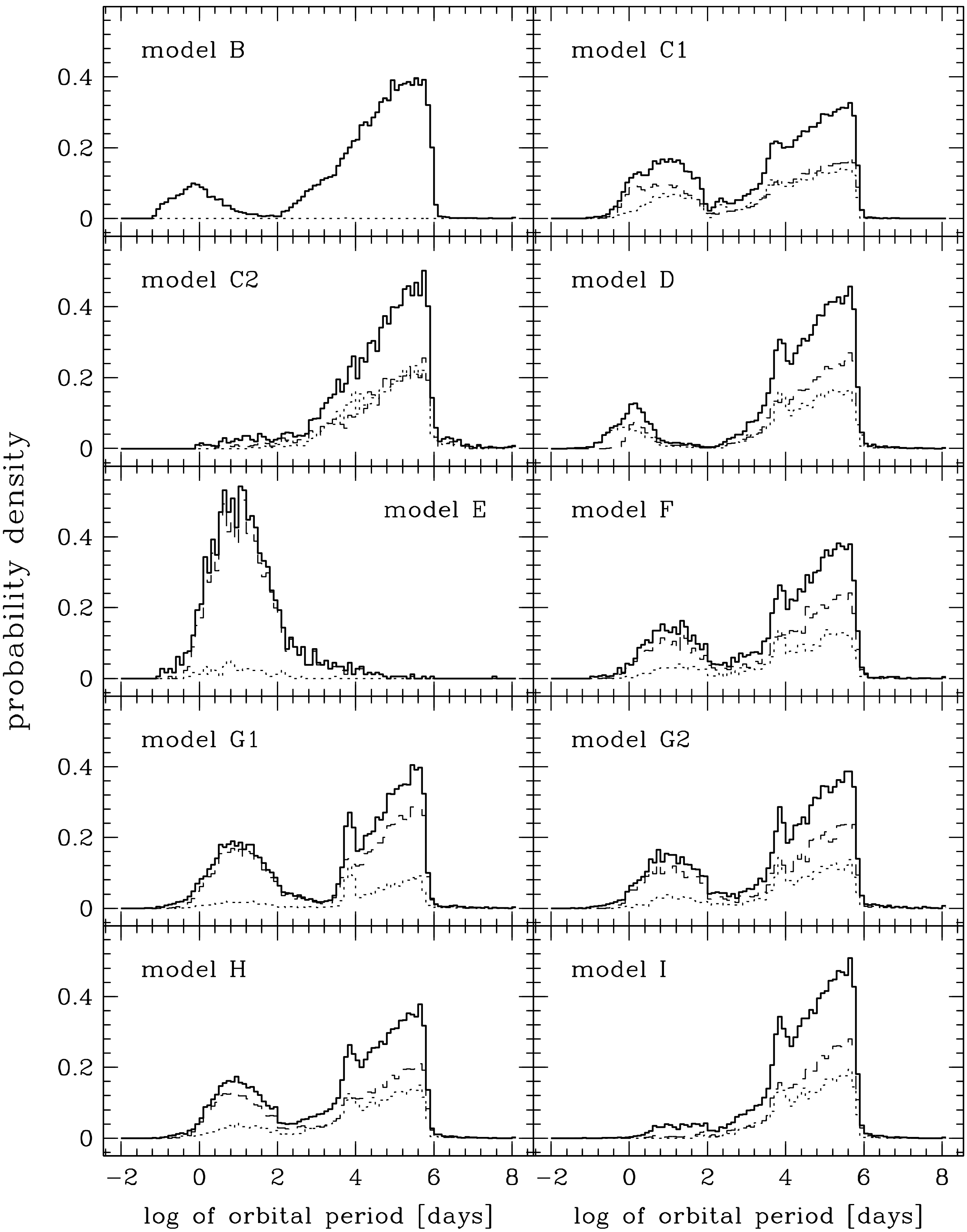

Fig. 3.— Period distribution of BH binaries (solid line) for different models, all at 11 Myr (dashed line: BH–MS binaries; dotted line: BH–BH binaries).

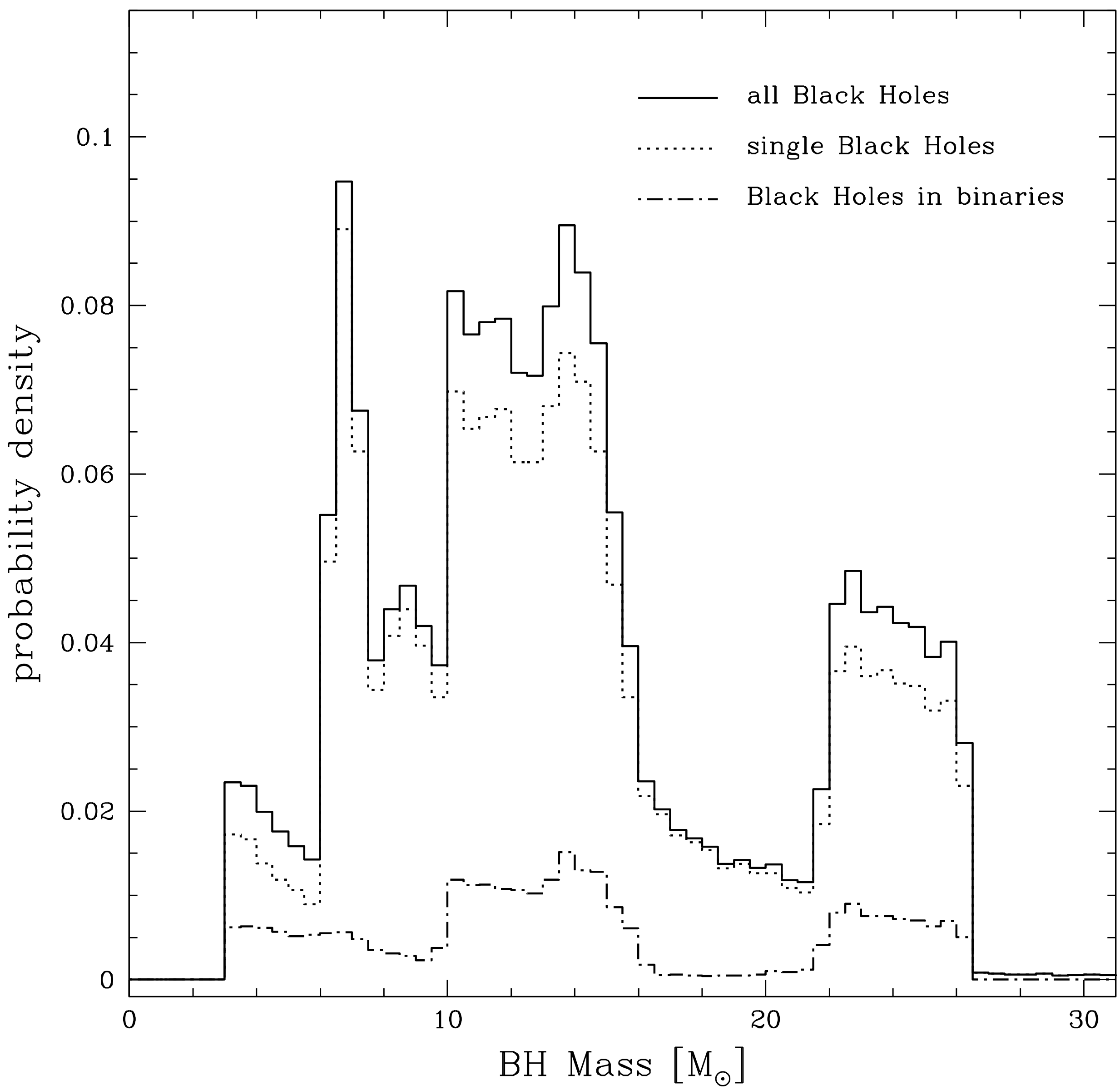

Fig. 4.— Mass distribution of BHs at 11 Myr (solid line) for standard model (A). Single BHs are shown with dotted line and BHs in binaries with dashed line. Normalized to total number of BHs (single and binaries); binwidth: $0.5 M_\odot$.

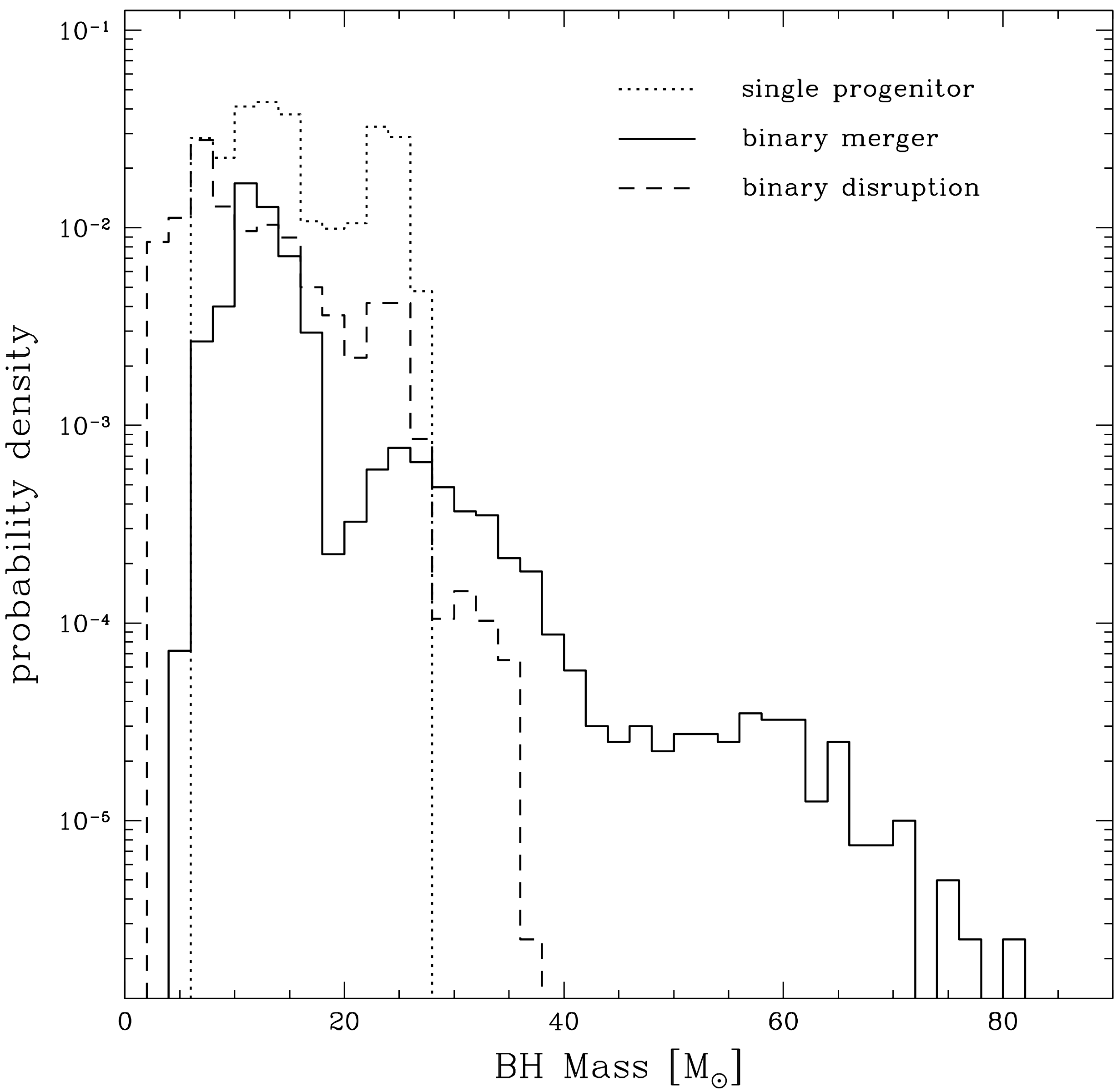

FIG. 5.— Mass distribution of various kinds of single BHs at 11 Myr in standard model (A). The dotted line shows BHs originating from primordial single stars; the dashed line represents single BHs from disrupted binaries; the solid line is for single BHs that are the remnants of merged binaries. Normalized to total number of BHs (single and binaries); binwidth: $2.0 M_{\odot}$.

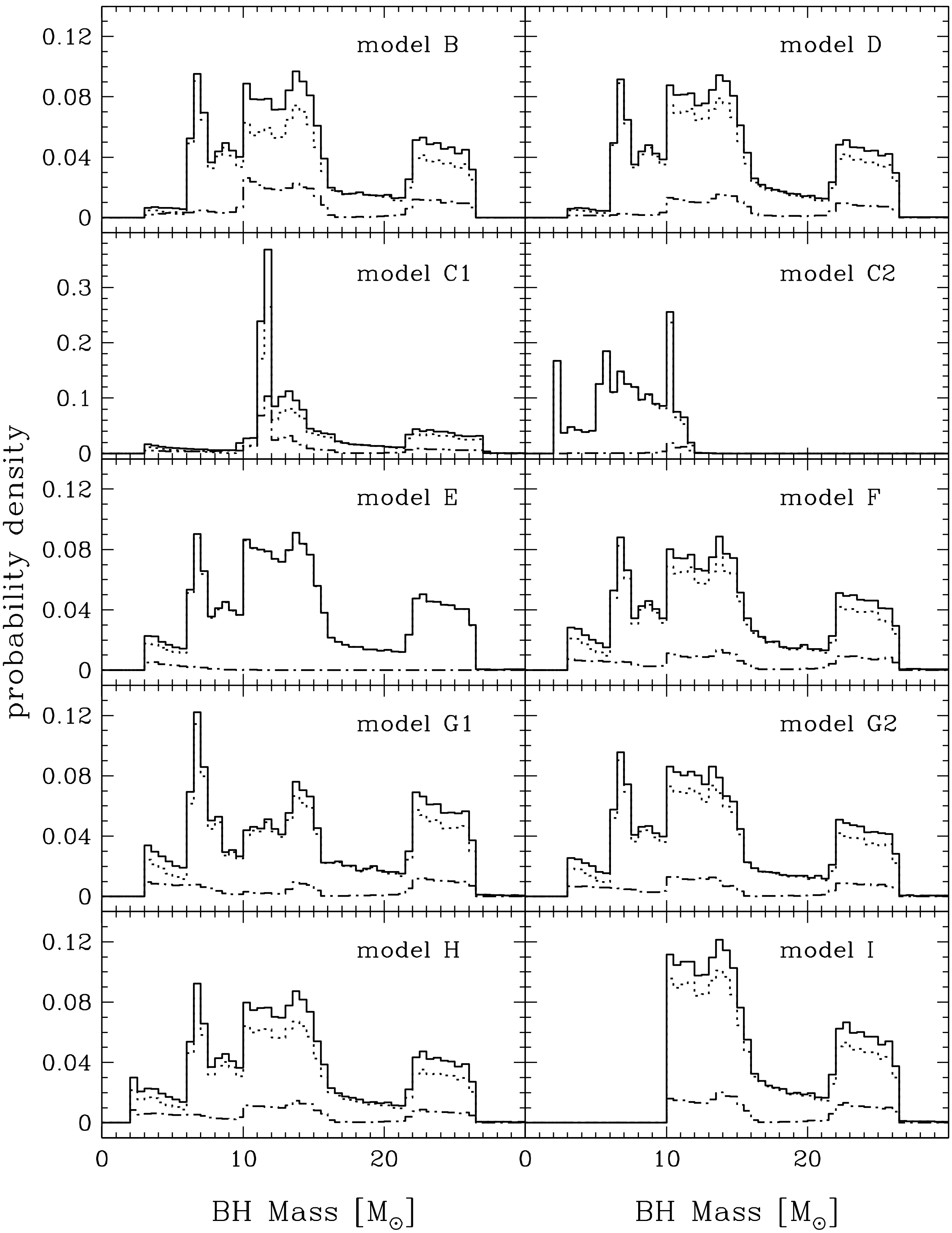

FIG. 6.— Mass distribution of BHs at 11 Myr for different models. Conventions are as in Fig. 4. Note that for Models C1 and C2 the vertical scale differs from the rest of the panels.

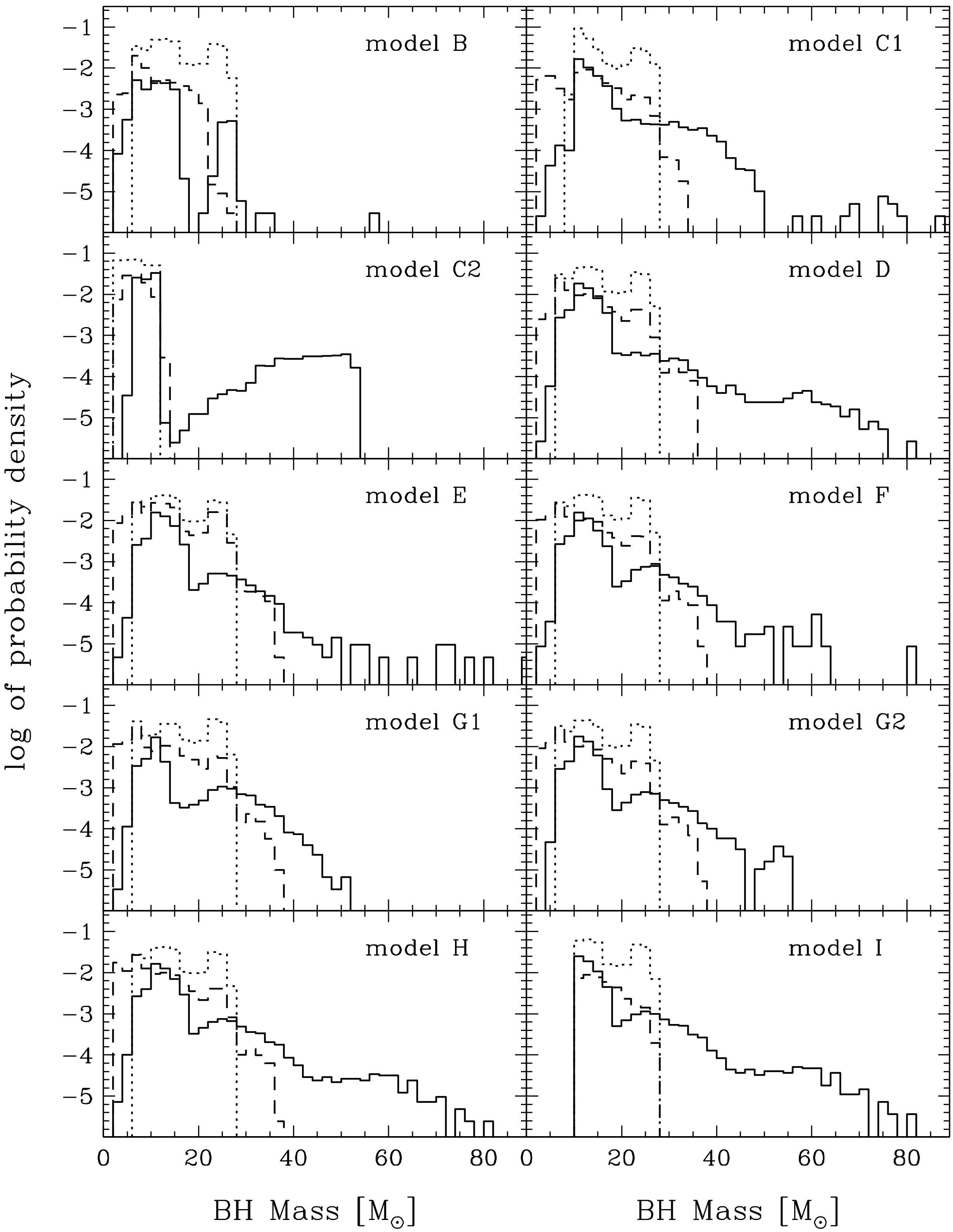

FIG. 7.— Mass distribution of various kinds of single BHs at 11 Myr for different models. Conventions are as in Fig. 5.